Supporting Information

Carbazole-2-Carbonitrile as an Acceptor in Deep-Blue Thermally Activated Delayed Fluorescence Emitters for Narrowing Charge-Transfer Emissions

Chin-Yiu Chan,[1,3] Yi-Ting Lee,[1,3] Masashi Mamada,[1] Kenichi Goushi,[1]*

*Youichi Tsuchiya,[1] Hajime Nakanotani,[1,2] and Chihaya Adachi [1,2]**

[1] *Center for Organic Photonics and Electronics Research (OPERA), Kyushu University, Motooka, Nishi, Fukuoka 819-0395, Japan*

[2] *International Institute for Carbon Neutral Energy Research (I2CNER), Kyushu University, 744 Motooka, Nishi, Fukuoka 819-0395, Japan*

[3]*These authors contributed equally to this work.*

E-mail:chinyiu.chan@opera.kyushu-u.ac.jp, adachi@cstf.kyushu-u.ac.jp

Synthesis

2,3,5,6-Tetrafluoro-5'-methyl-2'-(*p*-tolylamino)-[1,1'-biphenyl]-4-carbonitrile (**L1**)

Under nitrogen atmosphere, 4-bromotetrafluorobenzonitrile (254 mg, 1 mmol), 4-methyl-2-(4,4,5,5-tetramethyl-1,3,2-dioxaborolan-2-yl)-*N*-(*p*-tolyl)aniline (355 mg, 1.1 mmol), $Pd(PPh_3)_4$ (58 mg, 0.05 mmol) and potassium carbonate (414 mg, 3 mmol) were dissolved in degassed THF/water (3:1, v/v). The mixture was heated to reflux overnight. The reaction was slowly warmed to room temperature and stirred overnight. The reaction was extracted with dichloromethane three times and washed with deionized water, then the organic layer was evaporated to dryness. The crude was purified by column chromatography. Yield: 222 mg (60%). ^{1}H NMR (500 MHz, Acetone-d_6, 298 K, relative to Me_4Si): δ = 7.28 (s, 2H), 7.17 (s, 1H), 7.02 (d, 2H, 8.0 Hz), 6.83 (d, 2H, 8.0 Hz), 6.75 (s, 1H), 2.34 (s, 3H), 2.23 (s, 3H). ^{19}F NMR (471 MHz, Acetone-d_6): δ = −136.4 (m, 2H), −138.7 (m, 2H). MS (APCI) calcd. for $C_{21}H_{14}F_4N_2$: *m/z* = 370.3; found: 370.7 $[M]^+$.

1,3,4-Trifluoro-6-methyl-9-(*p*-tolyl)-9H-carbazole-2-carbonitrile (**CCN**)

Under nitrogen atmosphere, **L1** (370 mg, 1 mmol) was dissolved in dry *N*,*N*-dimethylformamide (30 mL) in a two-neck round-bottom flask equipped with a condenser. The reaction mixture was cooled to 0 °C, then NaH (40 mg, 1 mmol) was added. The reaction was then heated to 150 °C for 16 hours. The reaction was quenched with water and the precipitate was filtered off. The crude product was purified by column chromatography. Yield: 280 mg (80%). ^{1}H NMR (500 MHz, Acetone-d_6, 298 K, relative to Me_4Si): δ = 8.1 (s, 1H), 7.48–7.55 (m, 5H), 7.26 (d, 1H, 8.0 Hz), 2.57 (s, 3H), 2.51 (s, 3H). ^{19}F NMR (471 MHz, Acetone-d_6): δ = −127.9 (m, 1H), −147.5 (m, 1H), −149.9 (m, 1H). MS (APCI) calcd. for $C_{21}H_{13}F_3N_2$: *m/z* = 350.1; found: 350.1 $[M]^+$.

3CzCCN

Under nitrogen atmosphere, 9*H*-carbazole (501 mg, 3 mmol) was dissolved in dry *N*,*N*-dimethylformamide (30 mL) in a two-neck round-bottom flask equipped with a condenser. The reaction mixture was cooled to 0 °C, then NaH (120 mg, 3 mmol) was added. The reaction mixture was slowly warmed to room temperature and stirred for half an hour. After that, **CCN** (350 mg, 1 mmol) was added and the reaction was heated to 150 °C for 16 hours. The reaction was quenched with water and the precipitate was filtered off. The crude product was purified by column chromatography. Yield: 0.6 g (75%). ^{1}H NMR (500 MHz, CD_2Cl_2, 298 K, relative to Me_4Si): δ = 7.94–8.00 (m, 4H), 7.86 (d, 2H, 8.0 Hz), 7.50 (t, 2H, 7.5 Hz), 7.13–7.32 (m, 17H), 6.91 (d, 1H, 8.0 Hz), 6.55 (d, 2H, 8.0 Hz), 6.32 (d, 2H, 8.0 Hz), 6.19 (s, 1H), 2.10 (s, 3H), 1.96 (s, 3H). ^{13}C NMR (126 MHz, $CDCl_3$): δ = 143.1, 141.1, 140.2, 139.2, 138.0, 137.8, 131.6, 131.3, 131.2, 130.7, 130.0, 128.0, 128.0, 126.1, 126.0, 125.2, 125.2, 123.8, 123.8, 123.7, 123.7, 123.6, 120.5, 120.4, 120.2, 120.2, 120.0, 120.0, 119.9, 113.9, 113.4, 110.8, 110.4, 109.9, 109.7. MS (APCI) calcd. for $C_{57}H_{37}N_5$: *m/z* = 791.3; found: 791.3 $[M]^+$. Elemental analysis calcd. (%) for $C_{57}H_{37}N_5$: C 86.45, H 4.71, N 8.84; found: C 86.43, H 4.60, N 8.93.

3MeCzCCN

3MeCzCCN was synthesized accroding to the procedure of **3CzCCN**, except 3,6-dimethyl-9*H*-carbazole (585 mg, 3 mmol) was used instead of 9*H*-carbazole.Yield: 0.7 g (80%). ^{1}H NMR (500 MHz, $CDCl_3$, 298 K, relative to Me_4Si): δ = 7.65 (s, 2H), 7.58 (s, 2H), 7.51 (s, 2H), 7.19 (d, 2H, 8 Hz), 6.82–7.10 (m, 12H), 6.46 (d, 2H, 8.0 Hz), 6.26 (d, 2H, 8.0 Hz), 6.17 (s, 1H), 2.52 (s, 6H), 2.42 (s, 6H), 2.37 (s, 6H), 2.07 (s, 3H), 1.94 (s, 3H). ^{13}C NMR (126 MHz, $CDCl_3$): δ =142.9, 139.6, 139.2, 138.1, 137.8, 137.7, 132.0,

131.5, 131.0, 130.8, 130.3, 129.4, 129.3, 129.1, 128.0, 127.9, 127.0, 126.5, 126.4, 126.1, 124.3, 123.8, 123.6, 120.2, 120.0, 120.0, 119.8, 113.9, 113.4, 110.4, 110.2, 109.5, 109.3, 21.4, 21.4, 21.3. MS (APCI) calcd. for $C_{63}H_{49}N_5$: *m/z* = 875.4; found: 875.5 $[M]^+$. Elemental analysis calcd. (%) for $C_{63}H_{49}N_5$: C 86.37, H 5.64, N 7.99; found: C 86.37, H 5.54, N 8.06.

3PhCzCCN

3PhCzCCN was synthesized accroding to the procedure of **3CzCCN**, except 3,6-diphenyl-9*H*-carbazole (957 mg, 3 mmol) was used instead of 9*H*-carbazole.Yield: 0.97 g (78%). ^{1}H NMR (500 MHz, CD_2Cl_2, 298 K, relative to Me_4Si): δ = 8.27 (s, 2H), 8.14 (s, 2H), 8.03 (s, 2H), 7.84 (d, 6H, 8 Hz), 7.57–7.64 (m, 12H), 7.26–7.47 (m, 25H), 7.02 (d, 1H, 8.0 Hz), 6.85 (s, 1H), 6.70 (d, 2H, 7.5Hz), 6.43 (d, 2H, 7.5Hz), 2.16 (s, 3H), 2.10 (s, 3H). ^{13}C NMR (126 MHz, $CDCl_3$): δ = 143.3, 142.0, 141.8, 141.6, 141.1, 140.3, 139.6, 138.2, 137.9, 134.5, 134.3, 134.1, 132.2, 131.8, 131.3, 131.1, 130.2, 128.9, 128.8, 128.7, 128.5, 128.3, 127.4, 127.3, 127.3, 126.8, 126.7, 126.5, 126.3, 125.9, 124.9, 124.6, 124.6, 124.5, 123.6, 123.3, 120.5, 118.7, 118.5, 118.5, 114.0, 113.8, 111.8, 110.9, 110.6, 110.2. MS (APCI) calcd. for $C_{93}H_{61}N_5$: *m/z* = 1247.5; found: 1248.1 $[M]^+$. Elemental analysis calcd. (%) for $C_{93}H_{61}N_5$: C 89.47, H 4.92, N 5.61; found: C 89.38, H 4.75, N 5.65.

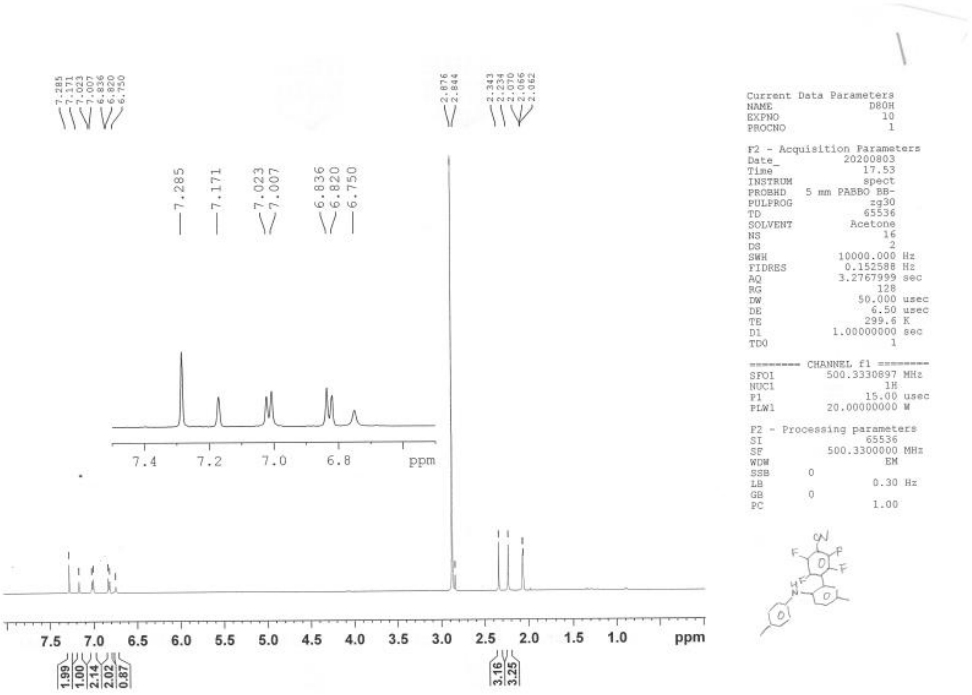

Figure S1. ^{1}H NMR spectrum of **L1**.

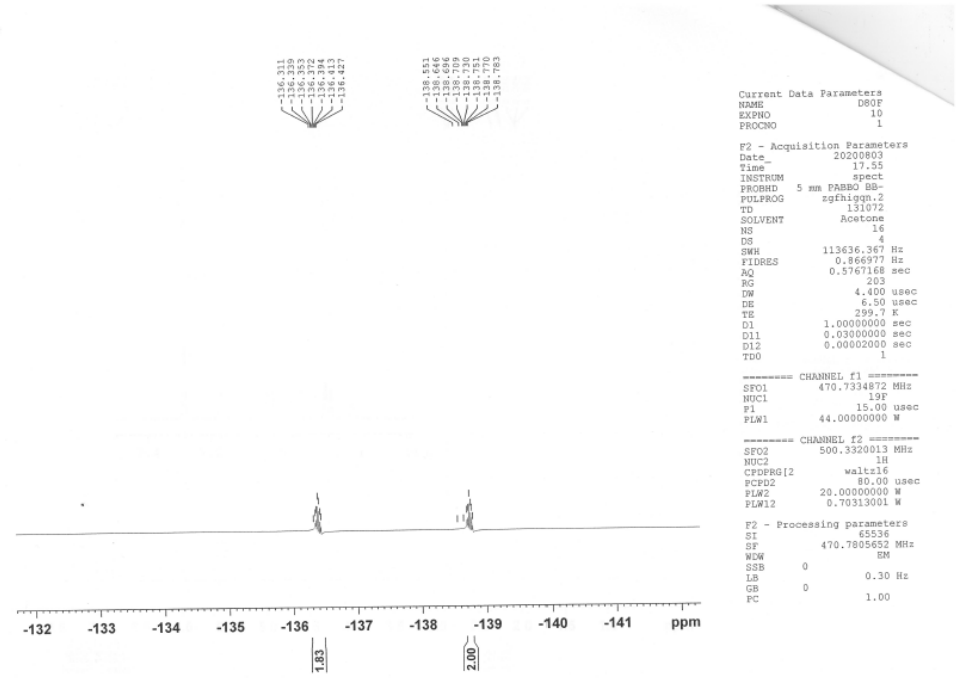

Figure S2. ^{19}F NMR spectrum of **L1**.

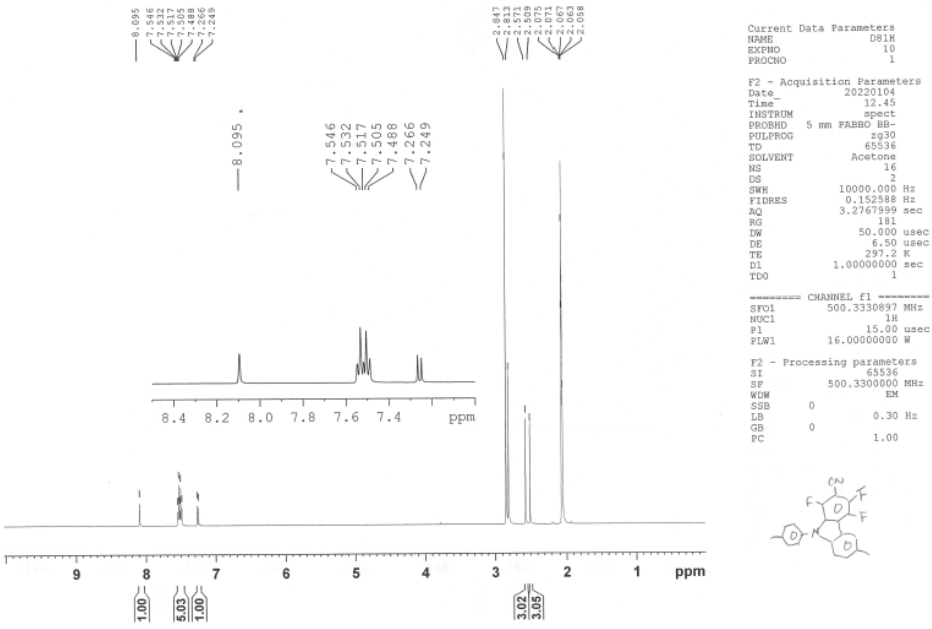

Figure S3. ^{1}H NMR spectrum of **CCN**.

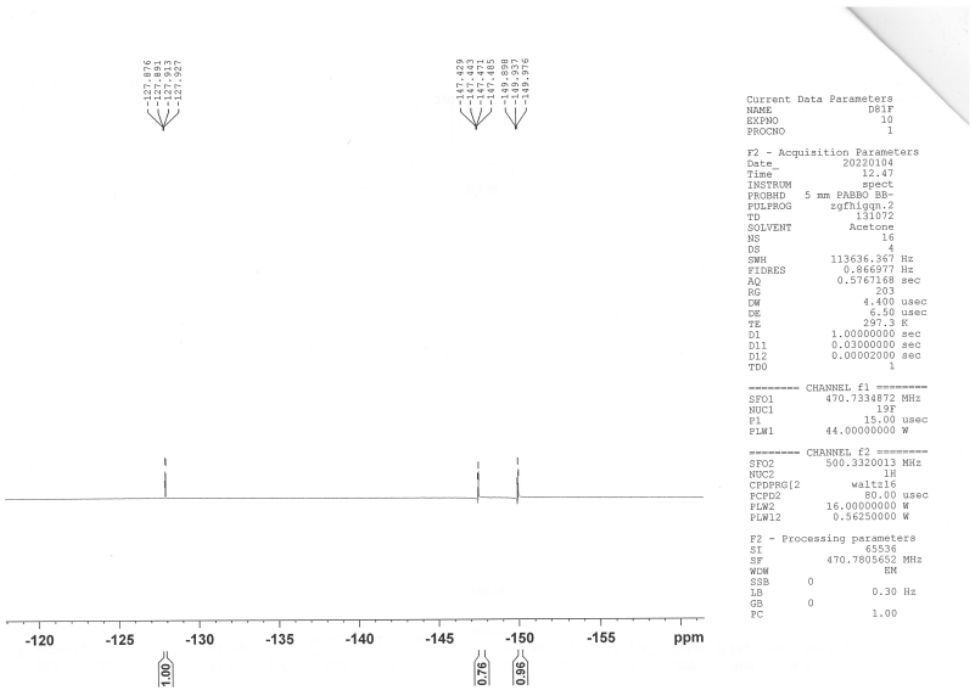

Figure S4. ^{19}F NMR spectrum of **CCN**.

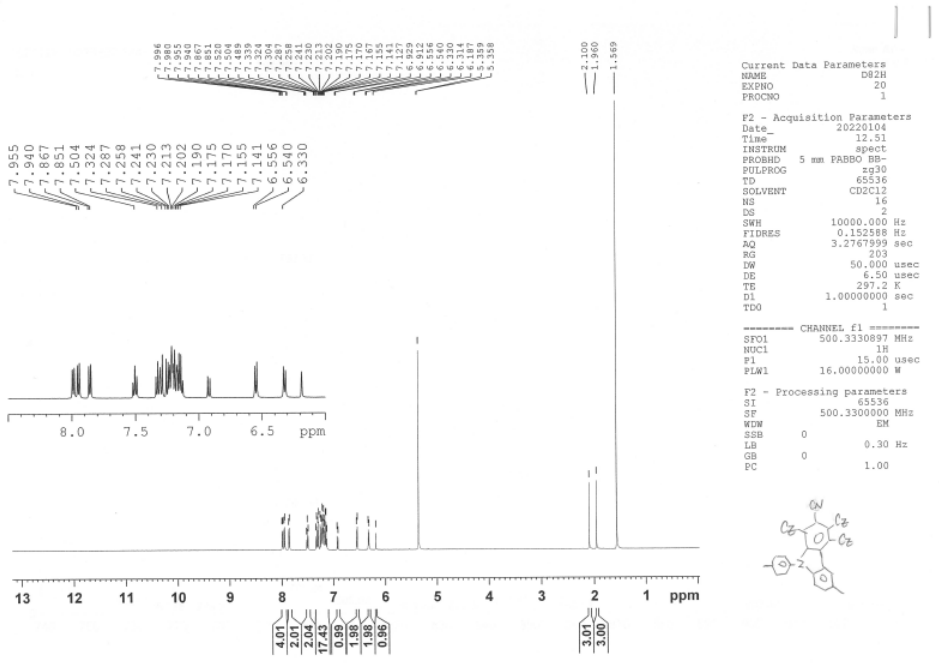

Figure S5. ^{1}H NMR spectrum of **3CzCCN**.

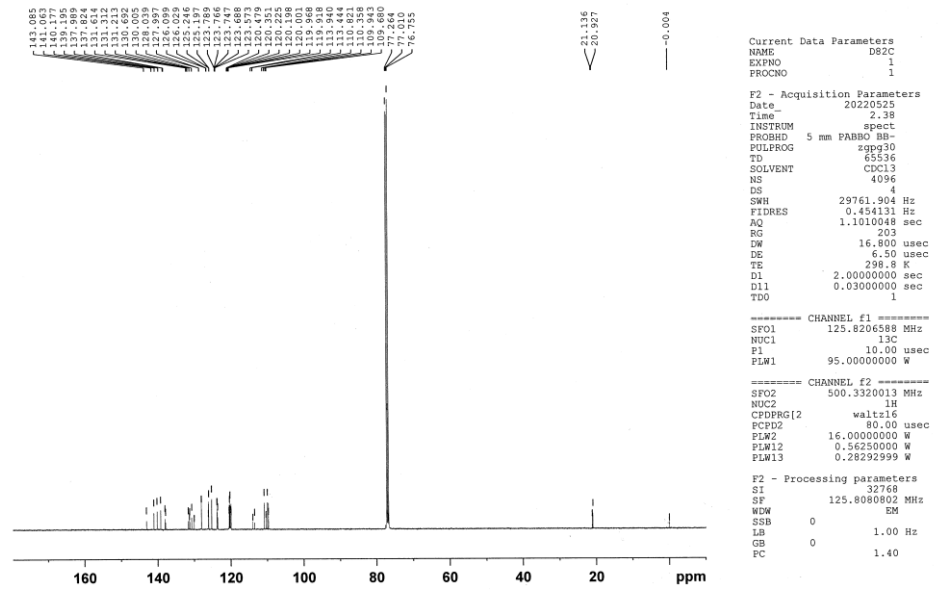

Figure S6. ^{13}C NMR spectrum of **3CzCCN**.

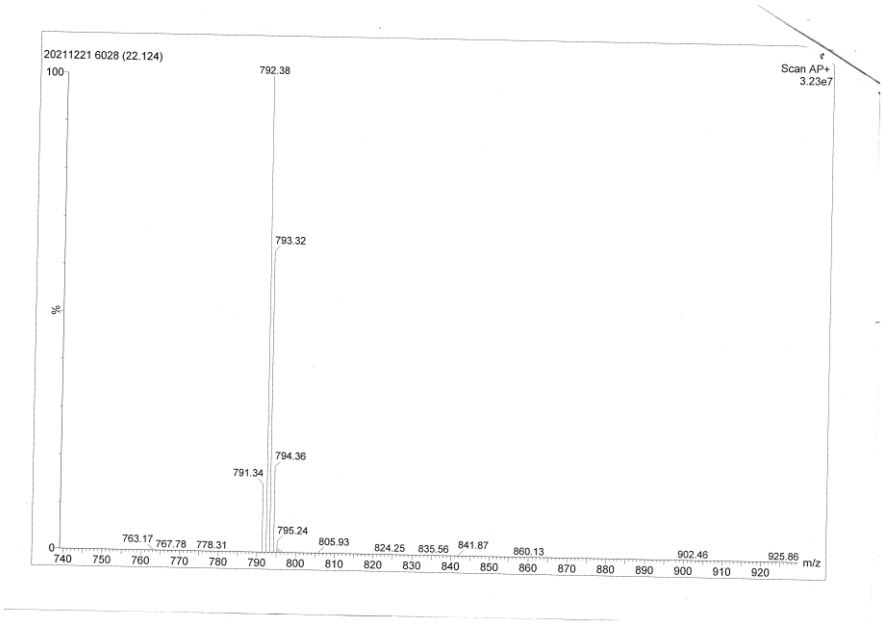

Figure S7. MS spectrum of **3CzCCN**.

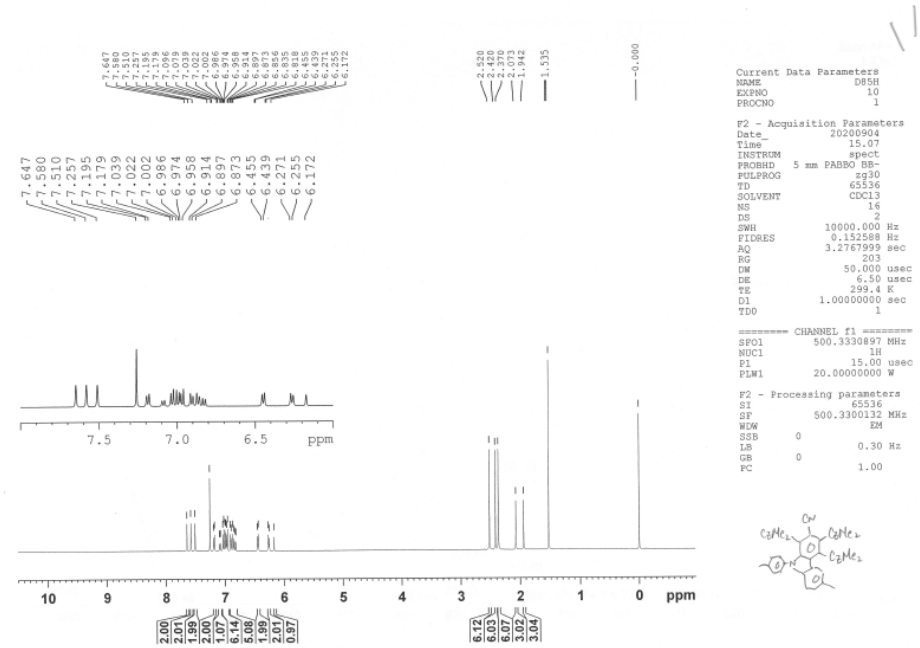

Figure S8. ^{1}H NMR spectrum of **3MeCzCCN**.

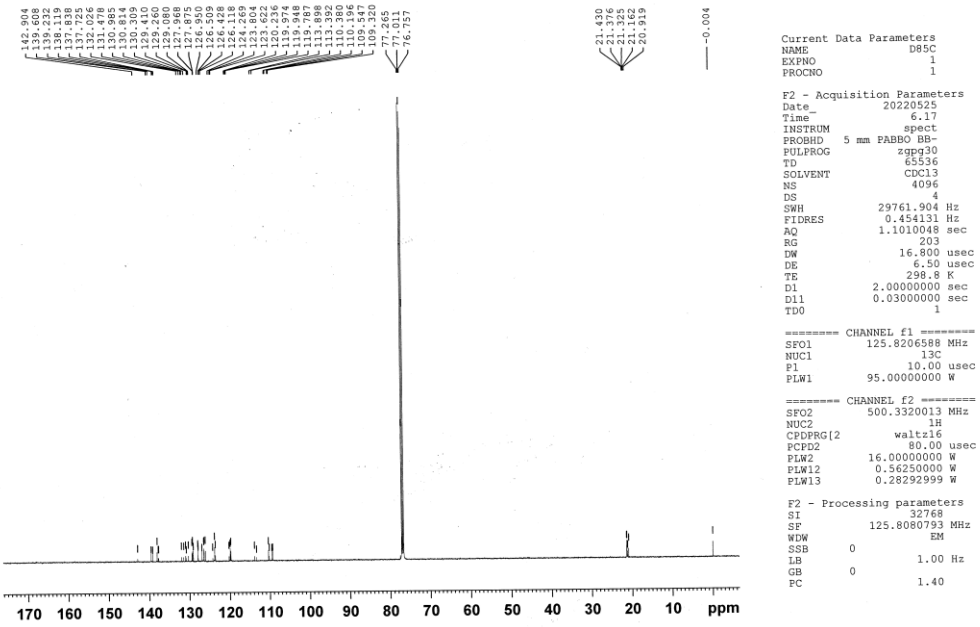

Figure S9. ^{13}C NMR spectrum of **3MeCzCCN**.

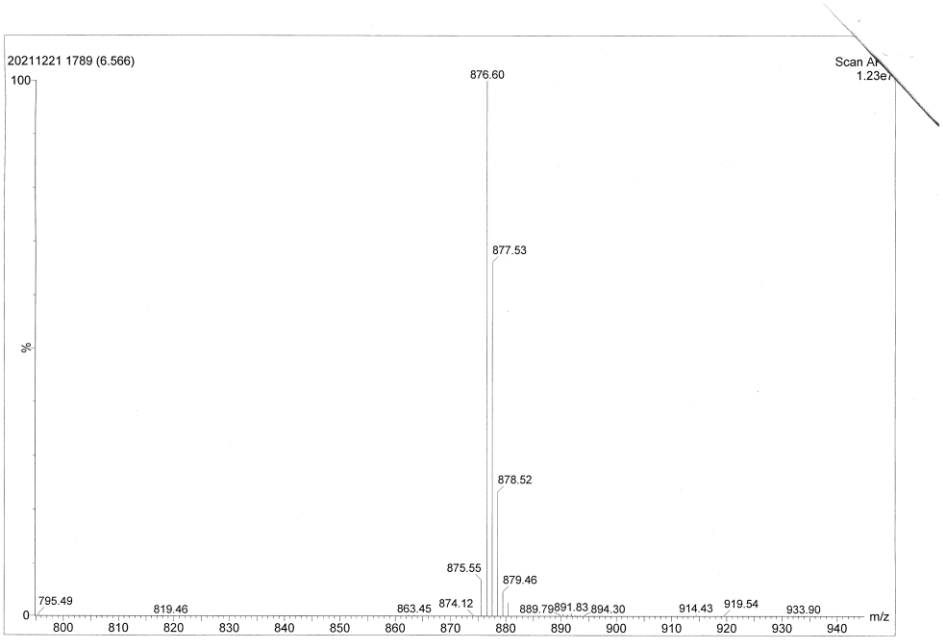

Figure S10. MS spectrum of **3MeCzCCN**.

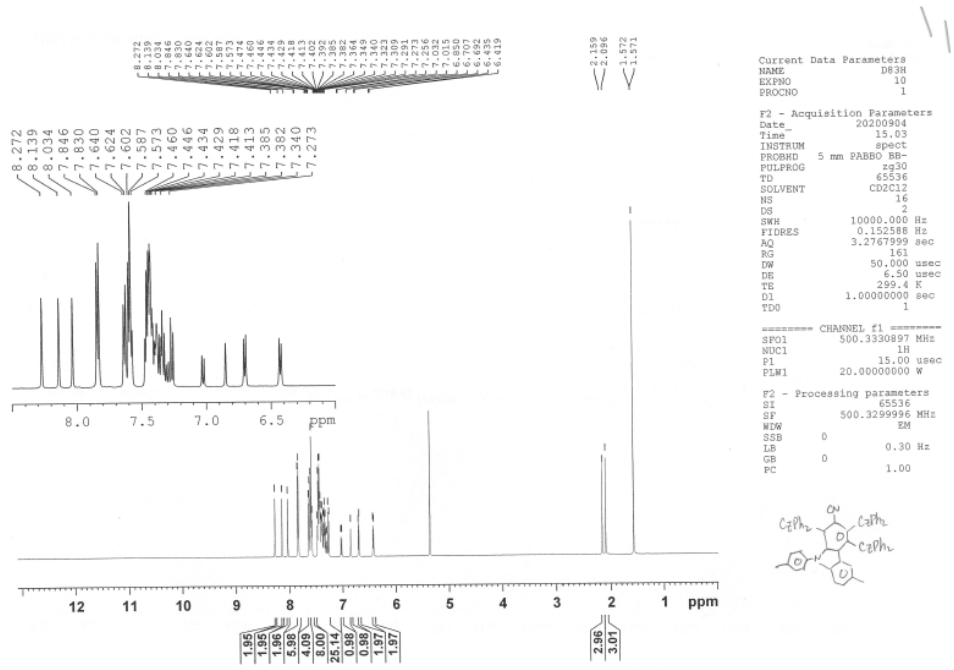

Figure S11. ^{1}H NMR spectrum of **3PhCzCCN**.

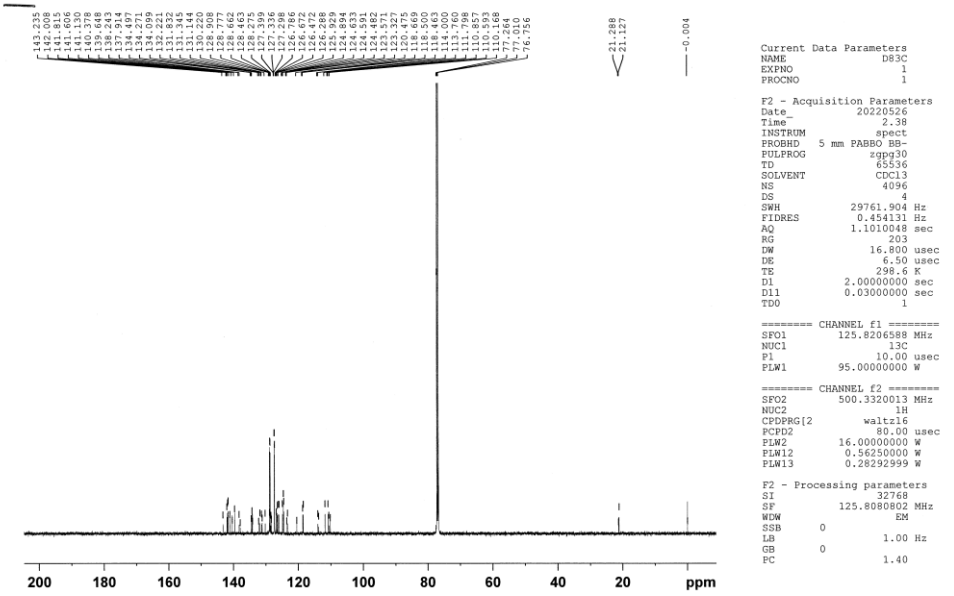

Figure S12. ^{13}C NMR spectrum of **3PhCzCCN**.

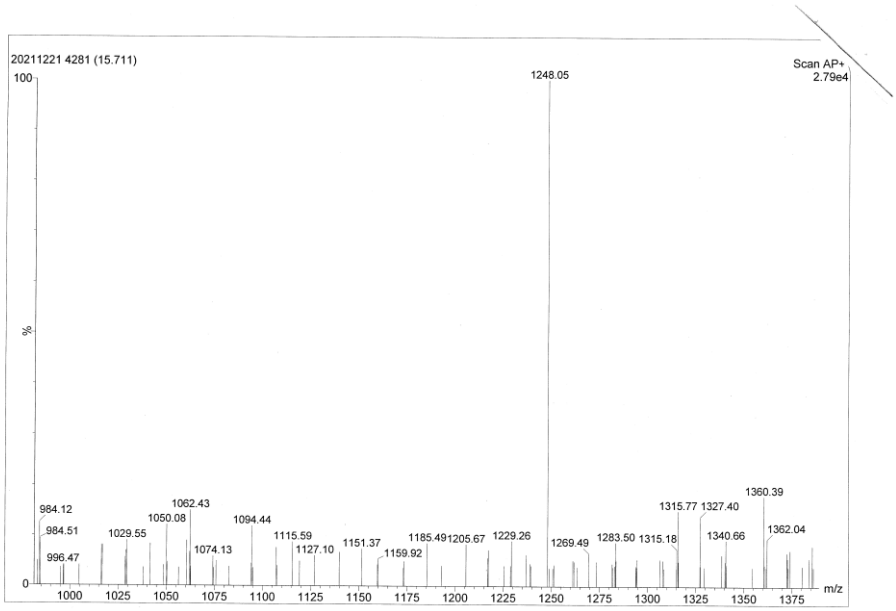

Figure S13. MS spectrum of **3MeCzCCN**.

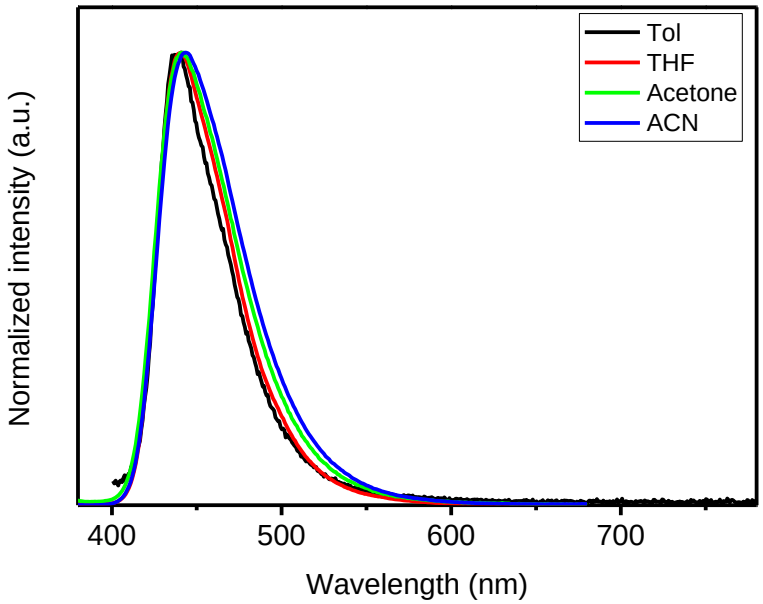

Figure S14. Solvatochromic study on emission of **3CzCCN**.

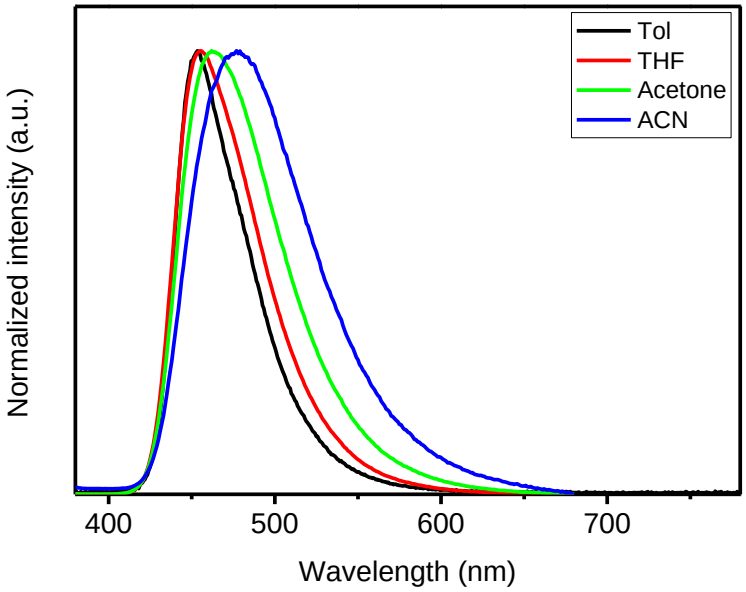

Figure S15. Solvatochromic study on emission of **3MeCzCCN**.

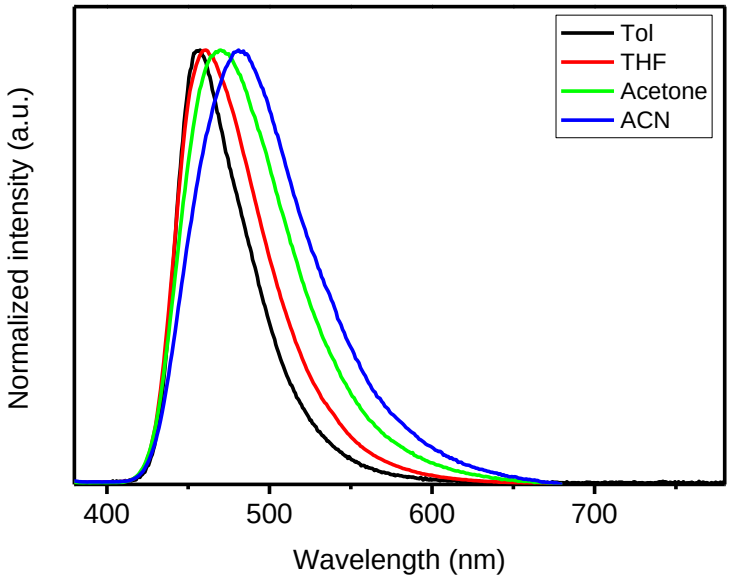

Figure S16. Solvatochromic study on emission of **3PhCzCCN**.

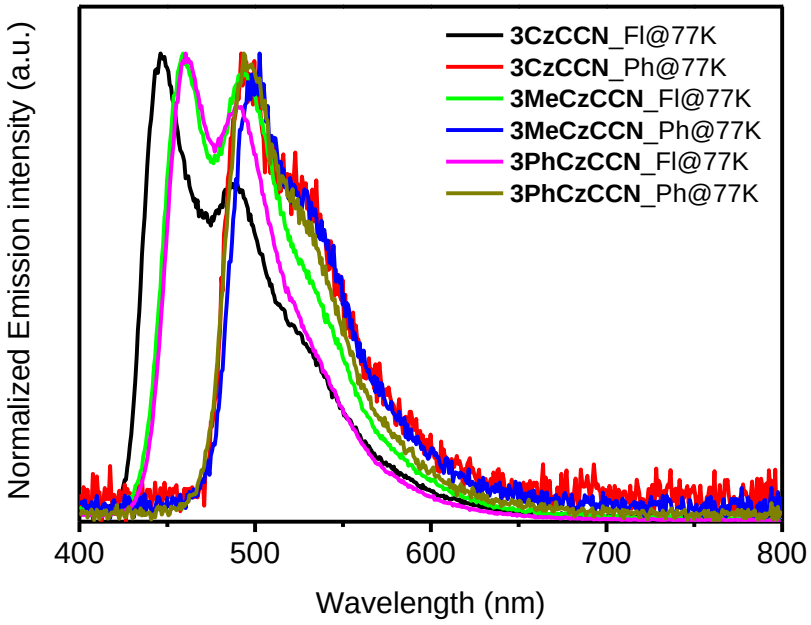

Figure S17. Fluorescence and phosphorescence spectra of 10 wt% of three emitters in mCBP doped films at 77 K.

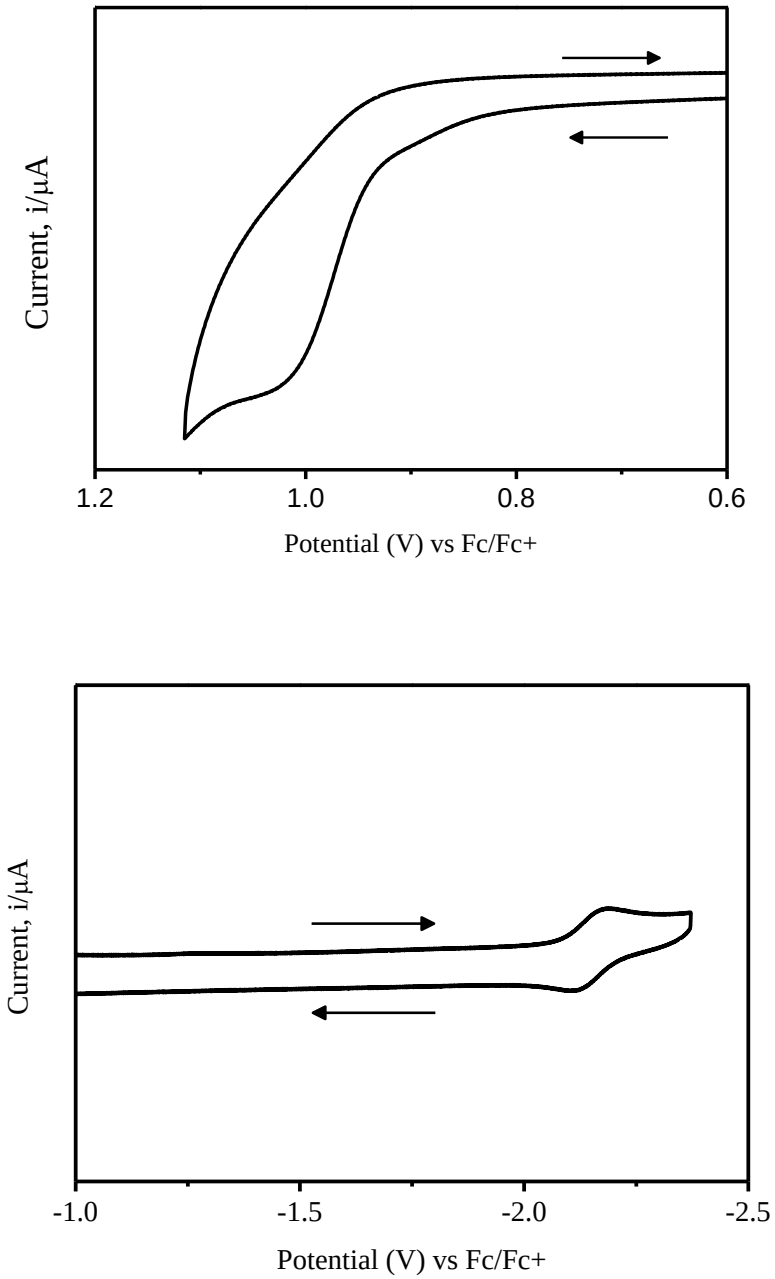

Figure S18. Cyclic voltammograms of **3CzCCN** in DMF.

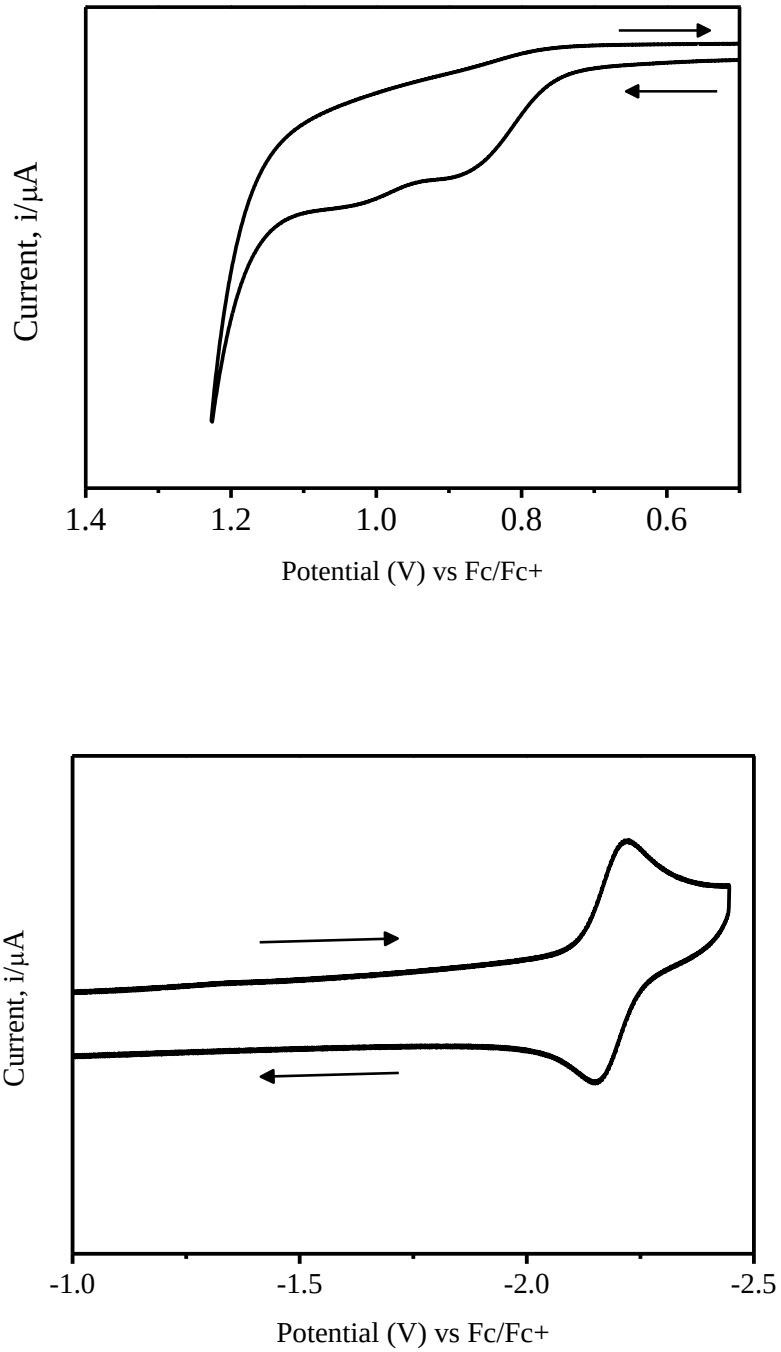

Figure S19. Cyclic voltammograms of **3MeCzCCN** in DMF.

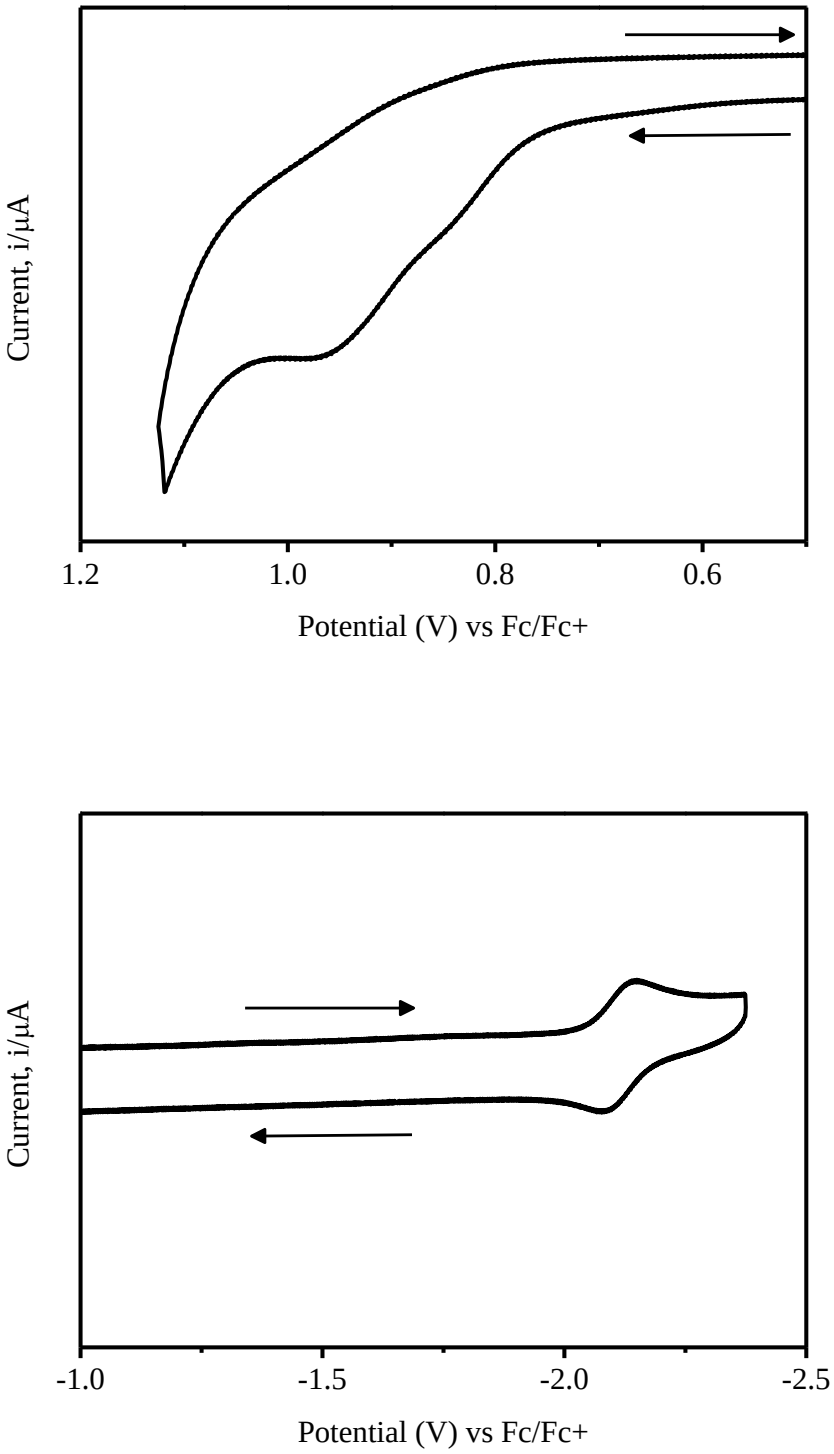

Figure S20. Cyclic voltammograms of **3PhCzCCN** in DMF.

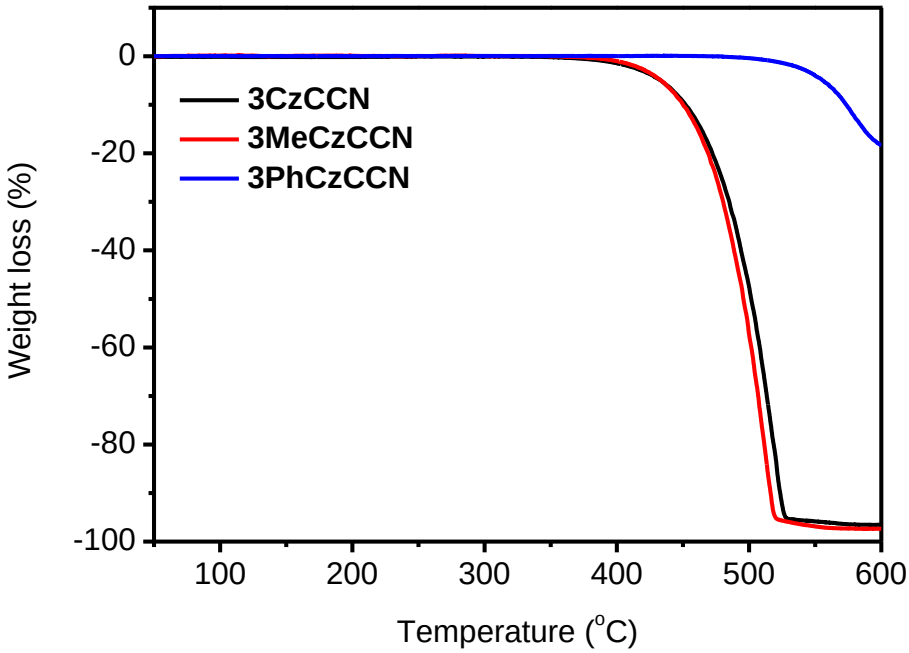

Figure S21. Thermogravimetric analysis of three emitters.

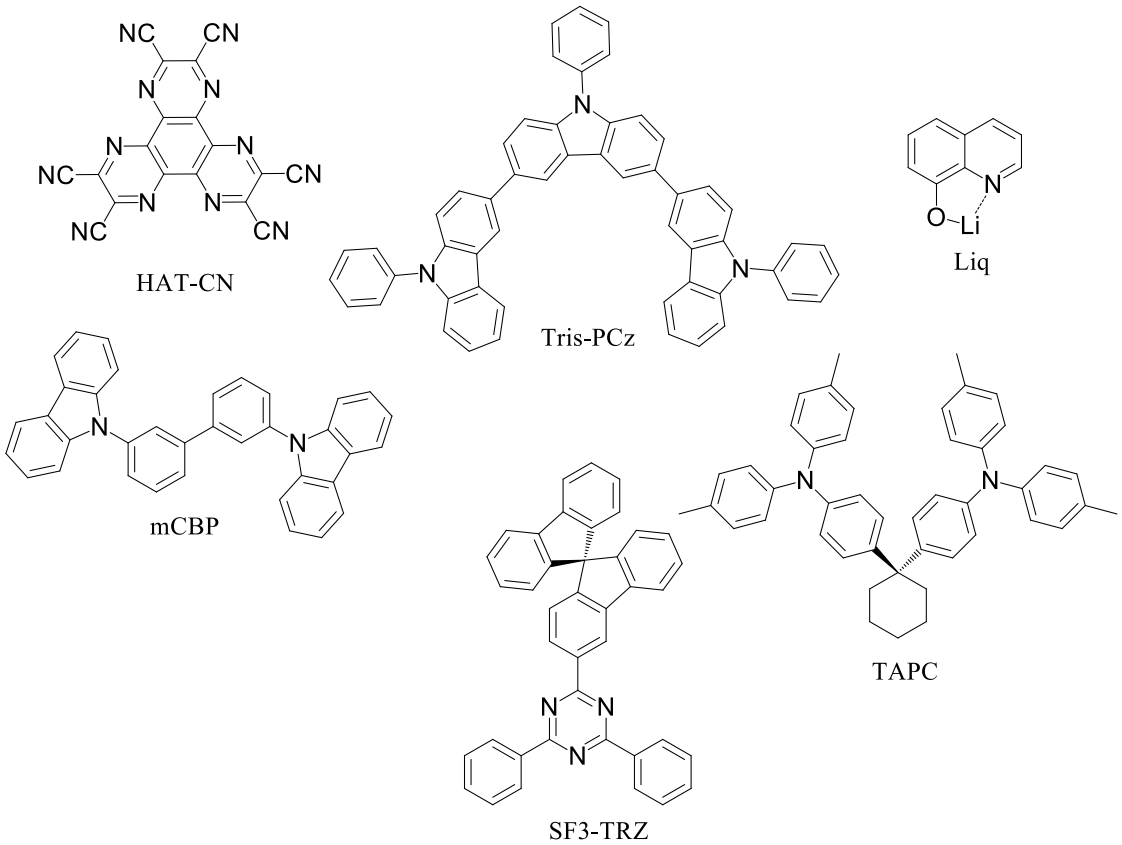

Figure S22. Materials used for blue CCN-based TADF OLEDs.

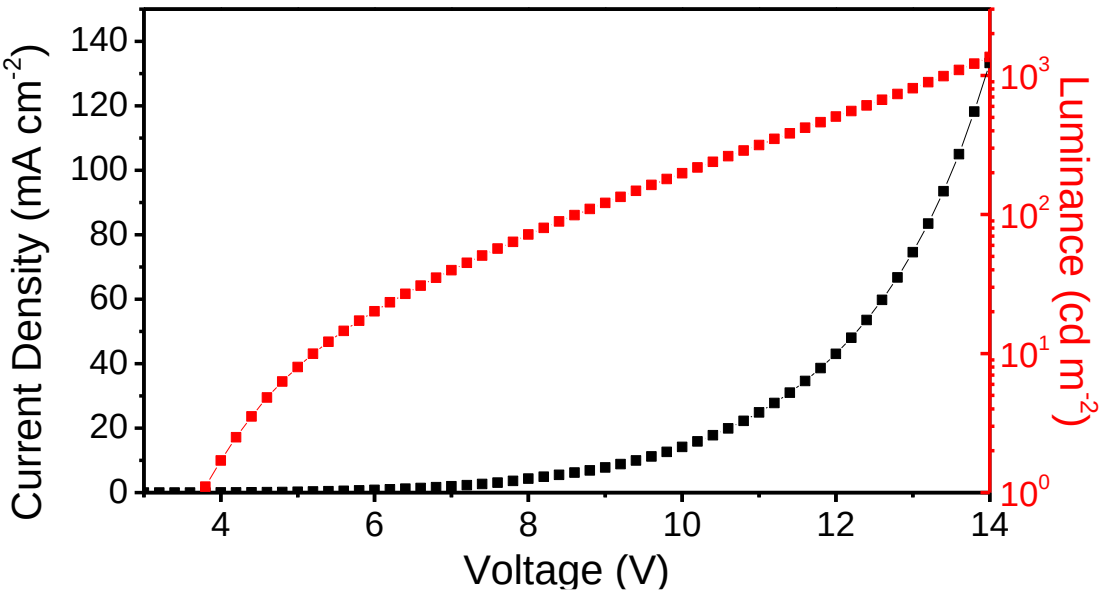

Figure S23. *J–V–L* characteristics of OLED based on **3CzCCN**.

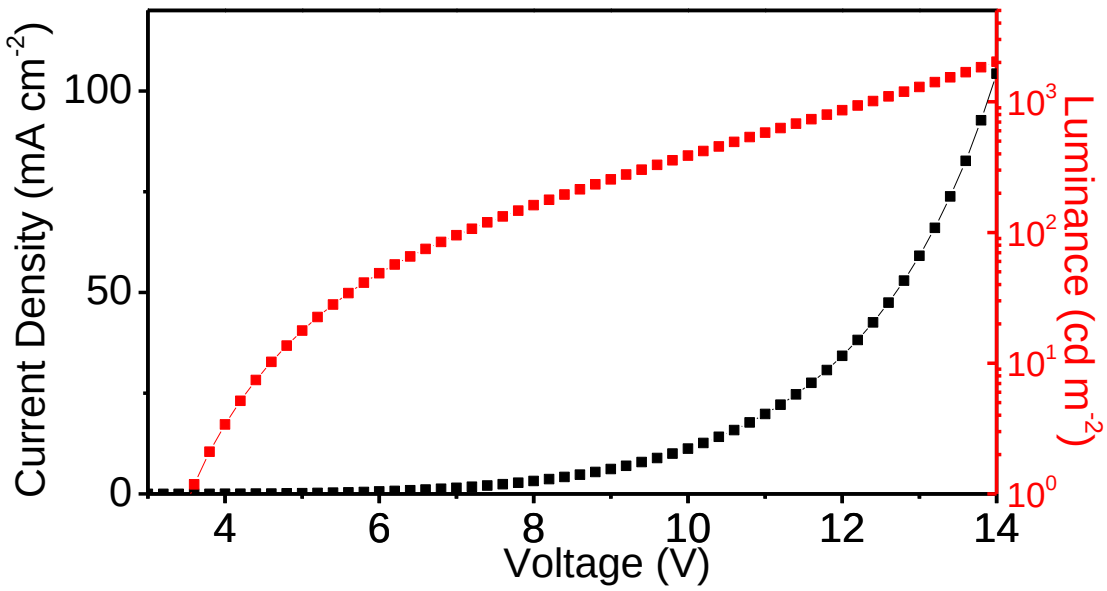

Figure S24. *J–V–L* characteristics of OLED based on **3MeCzCCN**.

.

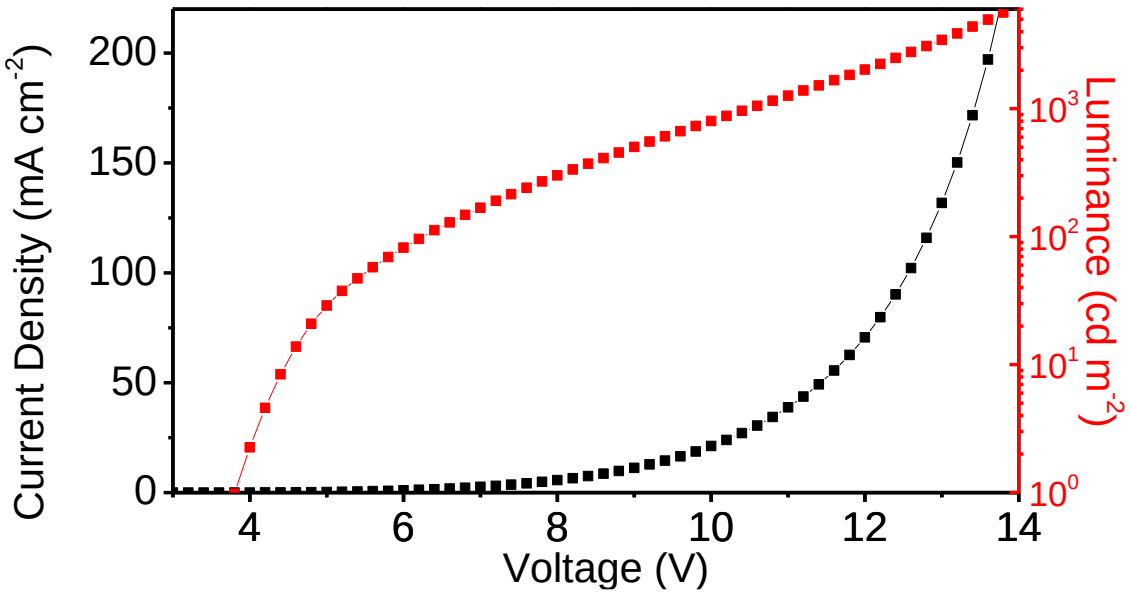

Figure S25. *J–V–L* characteristics of OLED based on**3PhCzCCN**.

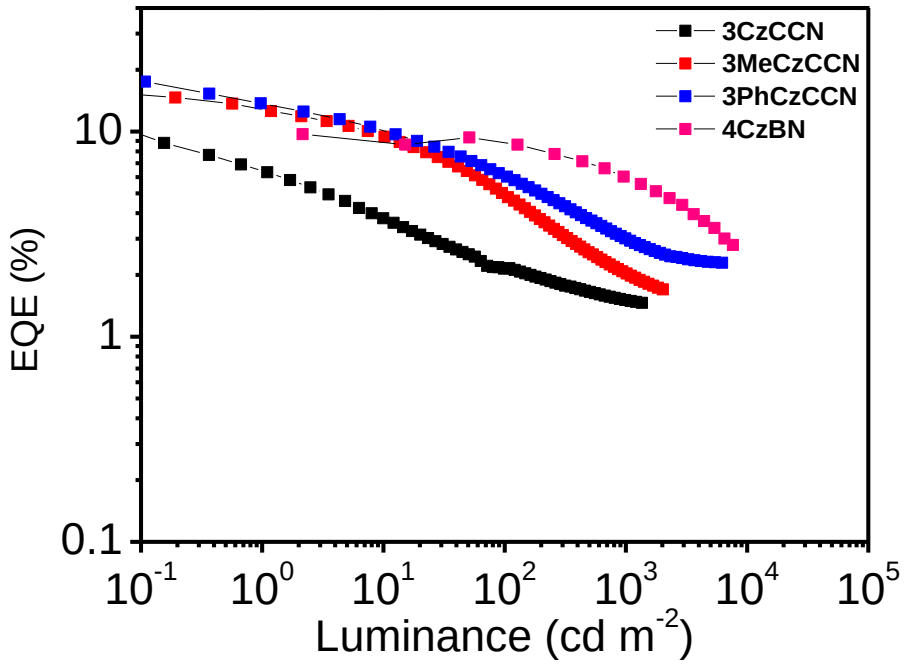

Figure S26. EQE versus luminance characteristic of devices **A**–**C** and **4CzBN**-based reference device.

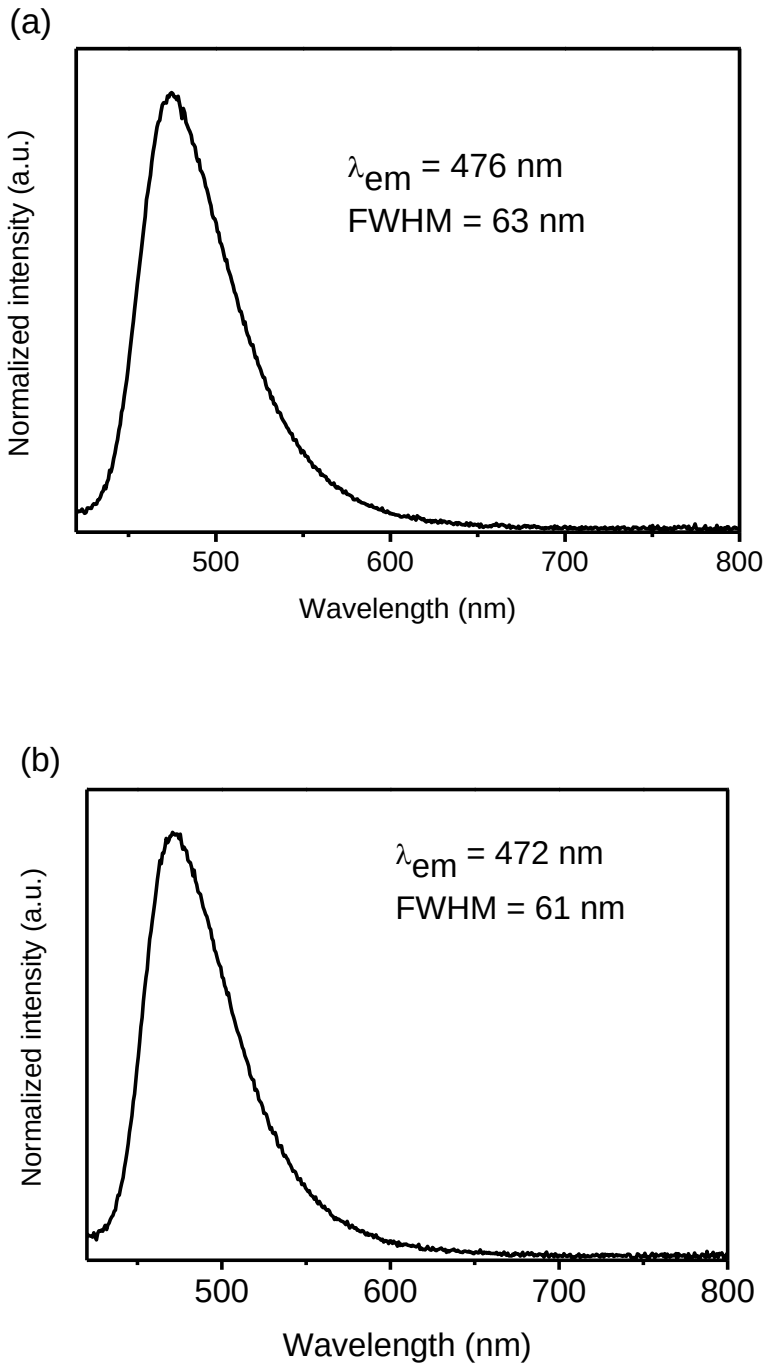

Figure S27. PL spectra of 10% of (a) **3MeCzCCN** and (b) **3PhCzCCN** doped in a PPT host.

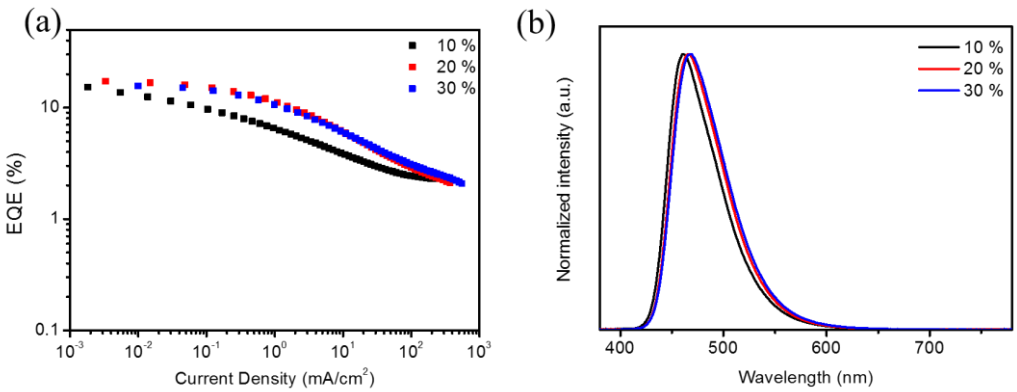

Figure S28. Device performance (a) EQE vs current density curves and (b) EL spectra of **3PhCzCCN**-based devices at different doping concentrations.

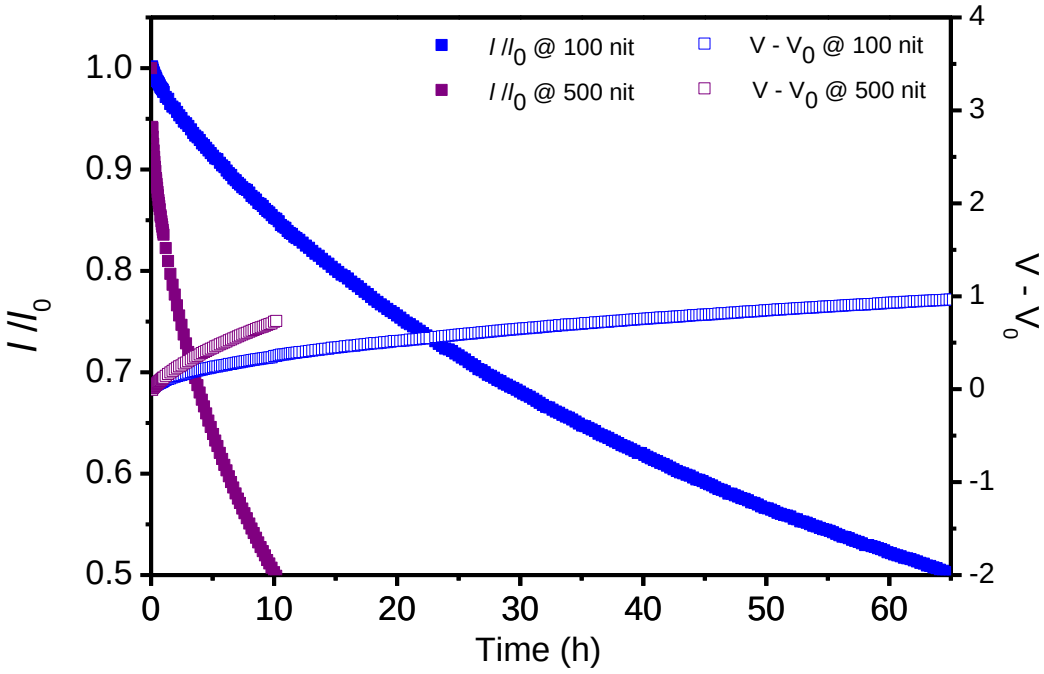

Figure S29. Device stabilities of OLEDs based on **3PhCzCCN** with an initial luminance of 100 or 500 nit.

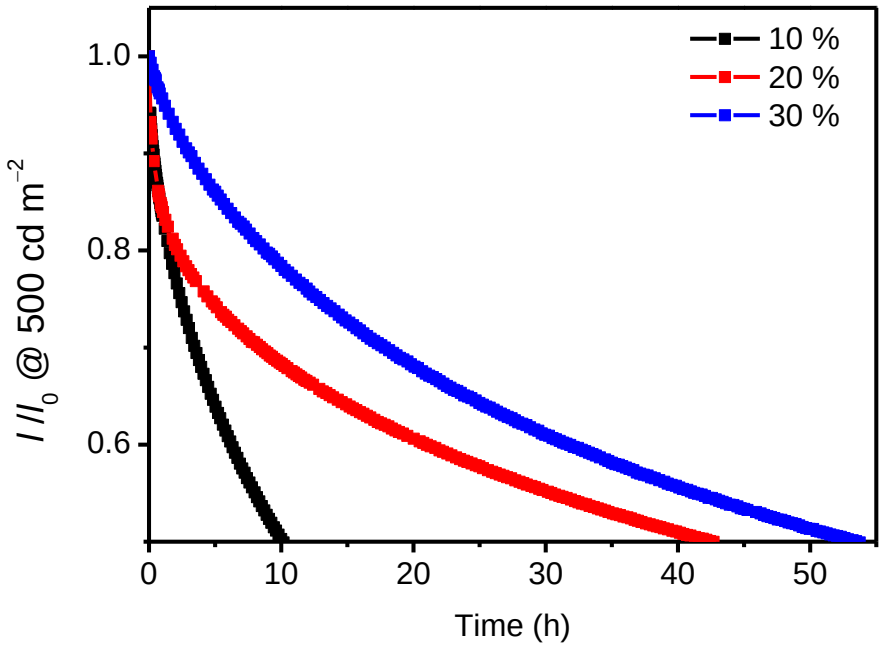

Figure S30. Device stabilities of OLEDs based on **3PhCzCCN** at different dopant concentrations with an initial luminance of 500 nit.

Table S1 Previous reports on narrow emission of non-MREs in toluene solutions with $\lambda_{max} \leq 460$ nm and FWHM ≤ 50 nm.

Emitter	λ_{max} (nm)	FWHM (nm)	ΔE_{ST} (eV)	Acceptor Type	Reference
3CzCCN	439	45	0.32	CCN	This work
3MeCzCCN	453	48	0.26	CCN	This work
3PhCzCCN	457	48	0.23	CCN	This work
TDBA-Ac	458	50	0.06	Boron	1
i-DMAc-C	414	49	0.31	Ketone	2
DMACN-B	430	29	0.27	Boron	3
PXZN-B	454	44	0.28	Boron	3
sAC-sDBB	453	50	0.15	Boron	4

Table S2. Summary of electronic energy (E) for **4CzBN** and **3CzCCN** at the S_0 and S_1 structures at the B3LYP/6-31G(d) level.

Compound	$E_{(S0@S0)}$ (a.u.)[a]	$E_{(S0@S1)}$ (a.u.)[a]	$E_{(S1@S0)}$ (a.u.)[b]	$E_{(S1@S1)}$ (a.u.)[b]
4CzBN	-2389.6042	-2389.5898	-2389.5007	-2389.5127
3CzCCN	-2468.2497	-2468.2394	-2468.1463	-2468.1561
3MeCzCCN	-2704.1688	-2704.1580	-2704.0697	-2704.0799
3PhCzCCN	-3854.6304	-3854.6207	-3854.5334	-3854.5429

[a]Electronic energy of S_0 at the optimized S_0 or S_1 structure, respectively; [b]Electronic energy of S_1 at the optimized S_0 or S_1 structure, respectively.

Table S3. Correlation between FWHM, $\Delta E(E_{(S1@S0)} - E_{(S1@S1)})$, and average change in bond length for **4CzBN** and **3CzCCN** at the B3LYP/6-31G(d) level.

Compound	FWHM in toluene (nm/meV)	ΔE (eV)[b]	Average change in bond length (Å)
4CzBN	63/375	0.3279	0.007884
3CzCCN	45/278	0.2685	0.006947
3MeCzCCN	48/277	0.2797	0.006828
3PhCzCCN	48/264	0.2577	0.004897

[a]FWHM in toluene solution; [b]$\Delta E(E_{(S1@S0)} - E_{(S1@S1)})$ from Table S2.

Table S4 Geometry changes in **4CzBN** and **3CzCCN** at S_0 and S_1 states.

Compound	**4CzBN**		**3CzCCN**		**3MeCzCCN**		**3PhCzCCN**	
S_0 in grey color S_1 in red color	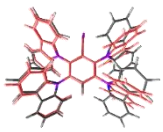		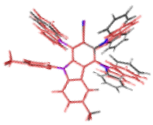		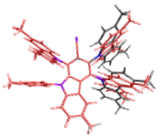		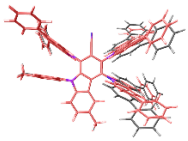	
Skeleton	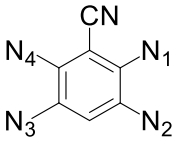		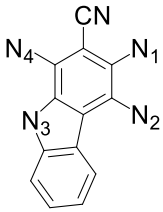					
Dihedral angle at S_0	N_1	64.1°	N_1	73.7°	N_1	74.5°	N_1	75.1°
	N_2	63.1°	N_2	74.3°	N_2	73.7°	N_2	74.0°
	N_3	63.1°	N_3	86.3°	N_3	85.6°	N_3	85.2°
	N_4	64.1°	N_4	88.0°	N_4	87.7°	N_4	87.0°
Dihedral angle at S_1	N_1	89.5°	N_1	90.0°	N_1	89.7°	N_1	83.5°
	N_2	89.7°	N_2	90.0°	N_2	89.7°	N_2	83.4°
	N_3	63.9°	N_3	90.0°	N_3	85.9°	N_3	83.1°
	N_4	66.9°	N_4	90.0°	N_4	88.0°	N_4	86.4°
Sum of changes in dihedral angle of 4 C-N bonds	55.7°		37.7°		31.7°		20.4°	

Table S5 Natural Transition Orbitals (NTOs) at singlet and triplet excited states of three CCN-based emitters.

	3CzCCN	**3MeCzCCN**	**3PhCzCCN**
Hole @S_1	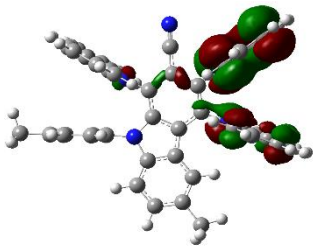	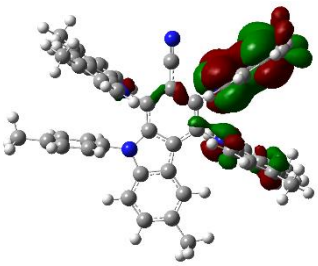	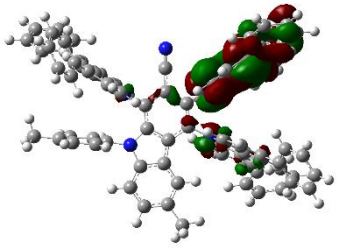
Electron @S_1	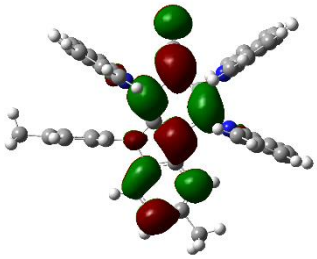	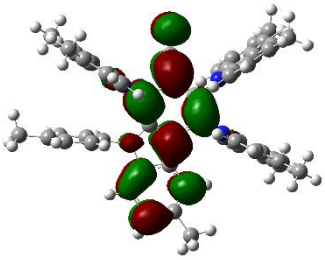	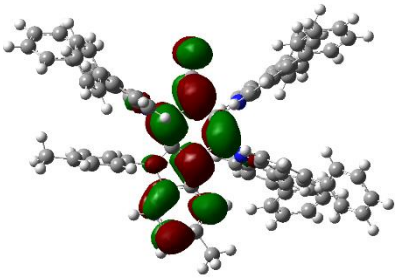
Hole @T_1	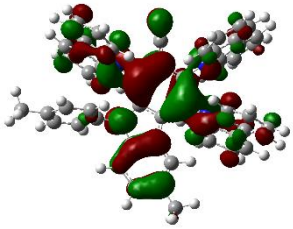	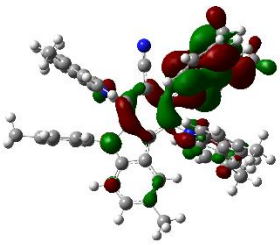	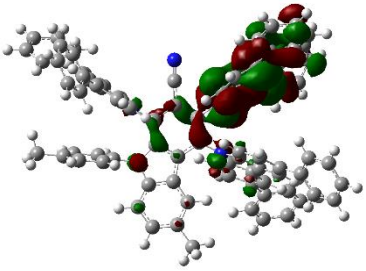
Electron @T_1	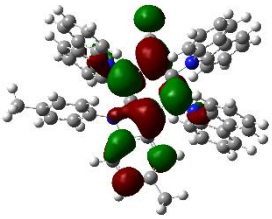	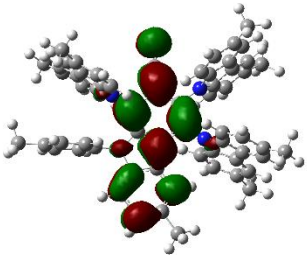	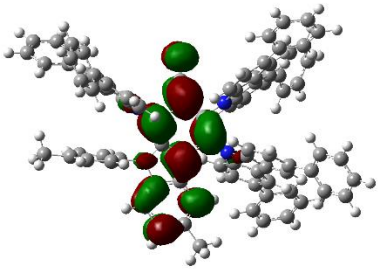

Table S6. Electrochemical properties of **3CzCCN, 3MeCzCCN** and **3PhCzCCN.**

Compound	E_{ox} [a] (V)	E_{red}[a] (V)	HOMO [b] (eV)	LUMO [b] (eV)
3CzCCN	+1.00	−2.14	−5.80	−2.66
3MeCzCCN	+0.87	−2.18	−5.67	−2.62
3PhCzCCN	+0.84	−2.11	−5.64	−2.69

[a]In DMF with 0.1 M [*n*Bu$_4$N]PF$_6$ as the supporting electrolyte and Fc/Fc$^+$ as the internal reference. [b]The HOMO and LUMO energies were determined using the equation of $E_{HOMO/LUMO} = -(E_{ox} / E_{red} + 4.8)$ eV,

Table S7. Thermal stability of **3CzCCN, 3MeCzCCN** and **3PhCzCCN** determined by thermogravimetric analysis.

Compound	T_{decomp} (°C)[a]
3CzCCN	433
3MeCzCCN	434
3PhCzCCN	555

[a]Decomposition temperature determined by 5 wt% loss.

References

1. D. H. Ahn, S. W. Kim, H. Lee, I. J. Ko, D. Karthik, J. Y. Lee, J. H. Kwon, *Nat. Photonics* **2019**, *13*, 540.
2. X. Cai, B. Gao, X.-L. Li, Y. Cao, S.-J. Su, *Adv. Funct. Mater.* **2016**, *26*, 8042.
3. A. Khan, X. Tang, X. Zhong, Q. Wang, S.-Y. Yang, F.-C. Kong, S. Yuan, A. Sandanayaka, C. Adachi, Z.-Q. Jiang, L.-S. Liao, *Adv. Funct. Mater*. **2021**, *31*, 2009488.
4. G. Xia, C. Qu, Y. Zhu, J. Ye, K. Ye, Z. Zhang, Y. Wang, *Angew. Chem. Int. Ed.* **2021** DOI: 10.1002/anie.202100423.